

Cite This: *ACS Earth Space Chem.* 2019, 3, 1302–1314

<http://pubs.acs.org/journal/aescq>

# Tracing Dissolved Lead Sources in the Canadian Arctic: Insights from the Canadian GEOTRACES Program

Manuel Colombo,\*†<sup>IP</sup> Birgit Rogalla,<sup>†</sup> Paul G. Myers,<sup>‡</sup> Susan E. Allen,<sup>†</sup> and Kristin J. Orians<sup>†</sup>

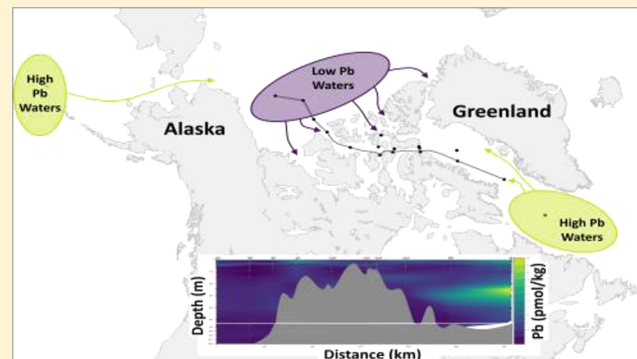
<sup>†</sup>Department of Earth, Ocean, and Atmospheric Sciences, University of British Columbia, Vancouver, British Columbia V6T1Z4, Canada

<sup>‡</sup>Department of Earth and Atmospheric Sciences, University of Alberta, 1-26 ESB, Edmonton, Alberta T6G2E3, Canada

## Supporting Information

**ABSTRACT:** This study addresses an important knowledge gap in the distribution of lead (Pb) in the Arctic Ocean, by presenting dissolved Pb concentrations from samples collected during the GEOTRACES Canadian cruise in 2015. Dissolved Pb showed an increase in concentration from the Canada Basin toward Baffin Bay and the Labrador Sea. Canada Basin was the most isolated region from anthropogenic Pb inputs with low background concentrations ( $1.4\text{--}6.2 \text{ pmol kg}^{-1}$ ) across most of the basin, although higher Pb features from the advection of Pacific-derived waters and sea ice meltwater were present. Likewise, high-Pb peaks ( $13.5\text{--}26.6 \text{ pmol kg}^{-1}$ ) along narrow isopycnal surfaces ( $\sigma_0$ ,  $27.4\text{--}27.6$ ) in Baffin Bay were attributed to the advection of North Atlantic waters spreading a high-Pb signature into the bay, contrasting with the low values ( $2.5\text{--}7.4 \text{ pmol kg}^{-1}$ ) present in the mixed layer, Arctic and Baffin Bay deep waters. The Labrador Sea, largely influenced by the recirculation of North Atlantic waters, had the highest Pb concentrations ( $\sim 17\text{--}34 \text{ pmol kg}^{-1}$ ) measured in this study. The Canadian Arctic Archipelago (CAA) represents a transition environment influenced by Arctic waters imprinting a low-Pb signature in the western CAA and the southern side of Parry Channel, while Baffin Bay waters prevailed in the eastern CAA recirculating westward along the northern side of Parry Channel and progressively losing their relatively high Pb signature. Extremely low concentrations were measured in Canada Basin and CAA waters, which reflect the remoteness of this region from anthropogenic inputs as well as the old ventilation age of deep waters' masses, providing a baseline for assessing future Pb studies. Finally, we successfully integrate modeling data with field observations demonstrating that dissolved lead, due to its distinctive anthropogenic signature in North Atlantic waters, can be a useful complementary tracer of water masses in the Canadian Arctic Ocean.

**KEYWORDS:** Lead Distributions, Geochemical Processes, Canadian Arctic Archipelago, Arctic Ocean Circulation, GEOTRACES



## INTRODUCTION

The geochemical cycle of lead (Pb) has been largely altered due to anthropogenic emissions, primarily by coal and leaded gasoline combustion, which have surpassed its natural sources.<sup>1–4</sup> The large spread of Pb contamination has been studied from numerous environmental matrices such as sediments,<sup>5–7</sup> ice cores,<sup>8,9</sup> and corals,<sup>10,11</sup> as well as with direct measurements of ocean waters (e.g., Boyle et al.<sup>12</sup> and references therein).

The North Atlantic Ocean was heavily impacted by Pb pollution due to early industrializing economies surrounding this basin, and it is certainly the most studied region with accurate Pb data from 1979 to the present.<sup>12–19</sup> Preanthropogenic (mid-1800s) surface Pb concentrations in the North Atlantic Ocean, reconstructed from the study of corals, ranged from 10 to 15  $\text{pmol kg}^{-1}$ , rising to about 90  $\text{pmol kg}^{-1}$  in the 1920s due to coal combustion and ore smelting.<sup>10,11</sup> After the 1940s, concentrations increased significantly, reaching a maximum value of about 200  $\text{pmol kg}^{-1}$  in the 1970s due to

the use of leaded gasoline. A steady decrease of dissolved Pb has been observed since the 1980s from the phasing out of leaded gasoline in 1970 and 1990 in North America and Europe, respectively.<sup>12,20</sup> The dissolved Pb surface concentrations in major ocean basins are decreasing toward preindustrial values ( $\sim 10\text{--}30 \text{ pM}$ )<sup>21</sup> due to the reduction of anthropogenic emissions. The higher concentrations, remnants from previous decades, have been declining due to scavenging removal and mixing with recently ventilated waters and have been deepening during thermocline ventilation, resulting in relatively high concentrations in intermediate waters of the North Atlantic Ocean.<sup>15,19,22,23</sup> Therefore, Pb distributions, despite not being conservative such as traditional tracers, e.g., salinity and temperature, lend complementary transient

Received: April 1, 2019

Revised: May 19, 2019

Accepted: May 21, 2019

Published: May 22, 2019

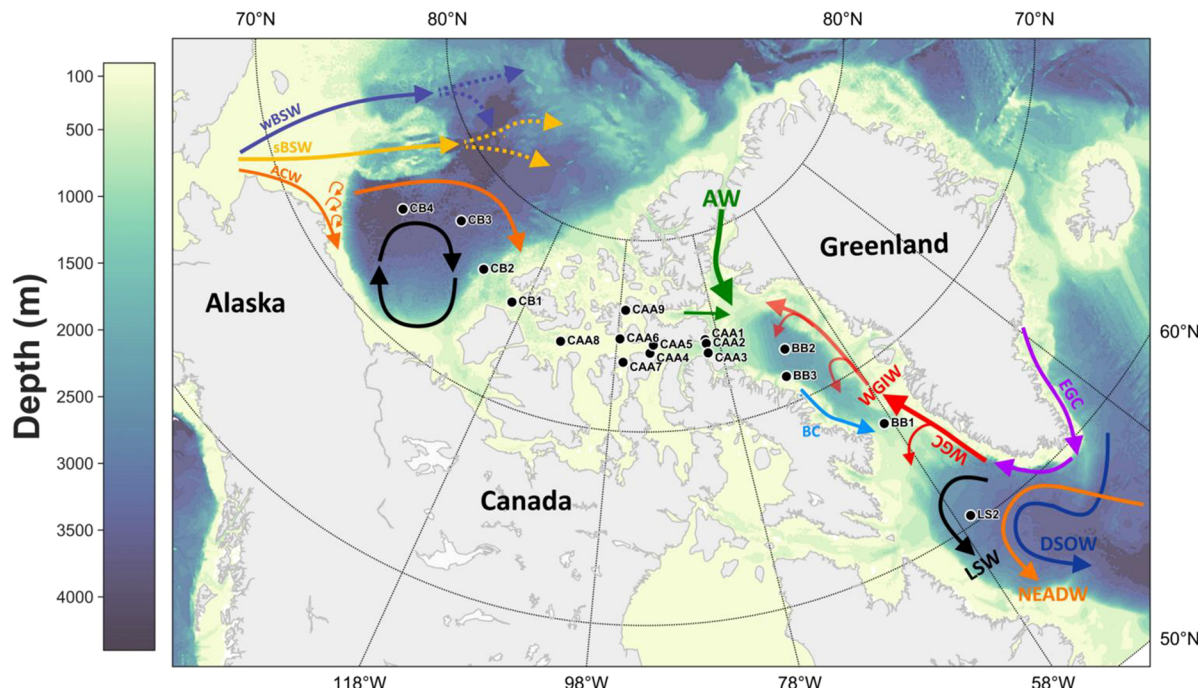


**Figure 1.** Sampled stations for lead during the Canadian Arctic GEOTRACES cruises (GN02 and GN03), bathymetry and schematic of Pacific-derived water circulation in the Canada Basin (after Timmermans et al.<sup>31</sup> and Kondo et al.<sup>44</sup>) and Baffin Bay and the Labrador Sea (after Yashayaev and Clarke,<sup>45</sup> Curry et al.,<sup>46</sup> and Lozier et al.<sup>42</sup>). CB, Canada Basin; CAA, Canadian Arctic Archipelago; BB, Baffin Bay; LS, Labrador Sea; ACW, Alaskan coastal water; sBSW, summer Bering Sea water; wBSW, winter Bering Sea water; AW, Arctic water; EGC, East Greenland current; WGC, West Greenland current; WGIW, West Greenland intermediate water; BC, Baffin current; LSW, Labrador Sea water; NEADW, Northeast Atlantic deep water; DSOW, Denmark Strait overflow water. For a detailed view of the Canadian Arctic Archipelago, including the main landmarks and straits, refer to Figure 6d.

information which can help trace and characterize water masses and their circulation.<sup>24</sup>

National and international research programs such as GEOTRACES ([www.geotrades.org](http://www.geotrades.org)) have been rapidly expanding our knowledge about the temporal and spatial distributions of Pb, and other trace elements, along with the internal cycling and equilibrium exchange of Pb between dissolved, colloidal, and particulate phases.<sup>25,26</sup> Recent studies report the distributions of Pb in the northwest Pacific Ocean,<sup>27</sup> eastern tropical Atlantic Ocean,<sup>24</sup> North Atlantic Ocean,<sup>19</sup> and the North Subarctic Atlantic including the Iceland Basin and the Irminger and Labrador Seas.<sup>23</sup> Nonetheless, the geochemistry of Pb in other regions, such as the Arctic Ocean, is still poorly characterized.

This work addresses this knowledge gap, unraveling the spatial and vertical distribution of dissolved Pb in the Canadian Arctic Ocean, a key pathway whereby the fresher and cooler Pacific-derived waters flow from the Canada Basin to the Labrador Sea. This study provides new insights into the sources and fate of Pb in the Canadian Arctic Ocean which, together with recent publications from the Subarctic region,<sup>23,27</sup> will help improve our understanding of the geochemical cycle of Pb in this changing environment.

## METHODS

**Study Area.** The circulation, water mass structure, and key features of the studied area are outlined below. The Canada Basin is strongly stratified, with a multilayered halocline (~30–400 m) which effectively insulates the polar mixed layer (PML; ~0–30 m) from the underlying heat of the Atlantic layer (~400–1500 m). Below the Atlantic layer (>1500 m) lies

the cold and more saline Canada Basin deep water.<sup>28–31</sup> The halocline in the Canada Basin is unique due to the presence of relatively fresh Pacific-origin waters and due to its spatial heterogeneity.<sup>29,32,33</sup> The Alaskan coastal water (ACW) and the winter Bering Sea water (wBSW) are advected from Bering Strait and modified during their flow across the Chukchi Sea, contributing to the upper and middle halocline assembly; the lower halocline consists mostly of Atlantic-origin waters,<sup>30,31,33</sup> Figure 1.

The Canadian Arctic Archipelago (CAA) is a complex network of islands and channels, connecting the Arctic Ocean to Baffin Bay. This shelf dominated region is an important export conduit of the fresh and nutrient rich Pacific-origin waters, enhancing productivity downstream,<sup>34–37</sup> and potentially impacting deep convection in the North Atlantic,<sup>36,38</sup> Figure 1.

Baffin Bay is connected to the Arctic Ocean through Lancaster Sound, Jones Sound, and Nares Strait, and to the Labrador Sea through the wider and deeper (300 km and 650 m) Davis Strait.<sup>36,39,40</sup> The overall circulation is cyclonic, with an Atlantic–Arctic-derived northward flow on the eastern side of Davis Strait, the West Greenland current (WGC), and a southward flow on the western side, the Baffin current. The Labrador Sea plays a key role in deep convection, contributing intermediate depth Labrador Sea water (LSW) to the Atlantic meridional overturning circulation.<sup>40–42</sup> The Labrador Sea subsurface (>500 m) circulation is cyclonic and consists of two components: the WGC and the Labrador current (LC). LSW is formed in late winter through deep convection, becoming colder, denser, thicker, and deeper, and is then isolated from

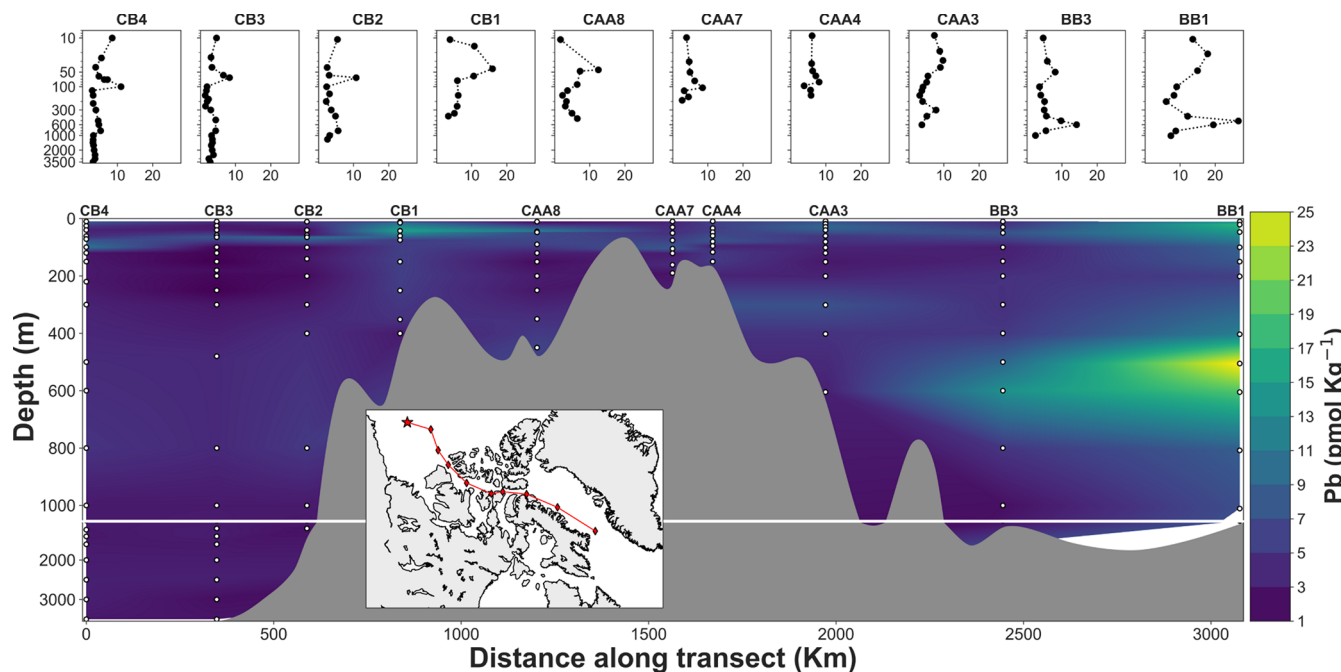


**Figure 2.** Interpolated contour section of dissolved Pb along the Canada Basin, the Canadian Arctic Archipelago, and Baffin Bay. Sampled depths are superimposed on the plot (white circles) and the individual Pb profiles are displayed above the contour plot. For those Pb samples for which replicate analyses are available, the error bars reflecting the standard deviation are smaller than the symbols. Stations sampled are displayed in the inset map, and the beginning of the transect is indicated by the red star. Note the break axis in the contour map and the logarithmic scale for the individual profiles. Stations were chosen to capture the flow of Arctic waters from the Canada Basin to Baffin Bay.

the surface.<sup>43</sup> A diagram displaying the main water masses discussed here is presented in Figure 1.

**Water Sampling and Analysis.** Seawater samples were collected during the Canadian Arctic GEOTRACES project aboard the CCGS *Amundsen* during two consecutive cruises (GN02 and GN03) from Labrador Sea to Beaufort Sea from Jul. 10 to Oct. 1, 2015. Samples were collected at 17 stations (Figure 1), targeting important physicochemical processes, water masses, and key locations (Supporting Information, Table S1). At each station, seawater was collected with the use of a powder coated trace metal rosette attached to a Kevlar line,<sup>47</sup> the rosette was equipped with 12 L, Teflon coated GO-Flo bottles (General Oceanics, Miami, FL, USA) and a SeaBird 911 CTD/SBE 43 oxygen sensor instrument package. Subsamples were filtered on board in a portable trace metal clean laboratory equipped with two HEPA filters, benches, and GO-Flo racks. To minimize external contamination, the samples were processed following the sampling and sample-handling protocols for GEOTRACES Cruises.<sup>48</sup> Briefly, seawater was filtered through 0.2 µm AcroPak Supor polyethersulfone capsule filters (VWR); subsamples (250 mL) were stored in Bel Art low-density polyethylene (LDPE) bottles and acidified to pH 1.8 using 500 µL of 6 M trace metal grade hydrochloric acid (HCl; Seastar Chemicals Inc., Sidney, Canada). LDPE bottles were thoroughly cleaned by soaking in successive baths at 60 °C of Extran liquid detergent (VWR), 6 M environmental grade HCl, and 0.7 M trace metal grade nitric acid (HNO<sub>3</sub>; Fisher Scientific, Ontario, Canada) for 1 day, 1 week, and 1 week, respectively, as recommended by the GEOTRACES protocol (<http://www.geotraces.org/>).

Dissolved Pb was preconcentrated 50-fold from 50 mL of acidified seawater using a modified magnesium-induced coprecipitation method and quantified by isotope dilution.<sup>49,50</sup>

The seawater sample was transferred into clean Falcon centrifuge tubes (Fisher Scientific, Ontario, Canada) by pouring directly from the bottle and allowed to equilibrate overnight with <sup>207</sup>Pb enriched spikes obtained from Oak Ridge National Laboratories. High-purity concentrated NH<sub>4</sub>OH (Seastar) was then added to precipitate the trace metals. After allowing ~10 min of Mg(OH)<sub>2</sub> precipitation to occur, the sample was mixed and centrifuged at 4,000 rpm for 2 min. The sample was then decanted and re-centrifuged under the same conditions. After being centrifuged, the pellet was redissolved in 1 mL of 1% HNO<sub>3</sub>. The analyses were conducted by high-resolution Thermo Finnigan Element2 inductively coupled plasma mass spectrometry in the Pacific Centre for Isotopic and Geochemical Research at the University of British Columbia. Brand new low-flow PFA-Teflon nebulizer (Elemental Scientific Inc., Omaha, NE, USA) and sample and skimmer cones (Fisher Scientific) were used for this study. To prevent contamination, the processing and analysis of the samples were conducted in class 1000 laboratories, maintained in an overpressure environment by HEPA filtered air and under class 100 laminar flow fume hoods. All of the plasticware used during the analysis were cleaned as previously described.

The advantage of this method lies in the low-reagent blank used, which minimizes the potential for contamination. During the analysis, procedural blanks and quality control spikes (acidified Milli-Q water equilibrated with <sup>207</sup>Pb enriched and natural Pb standards) were routinely run to ensure quality of the measurements. Additionally, duplicate seawater samples were run for each profile approximately every six samples. All sample concentrations reported here are corrected for the analytical blank by subtracting the average blank on the corresponding analytical day. The counts per second (cps) of the blanks run during the analysis (*n* = 56) were 549 ± 263,

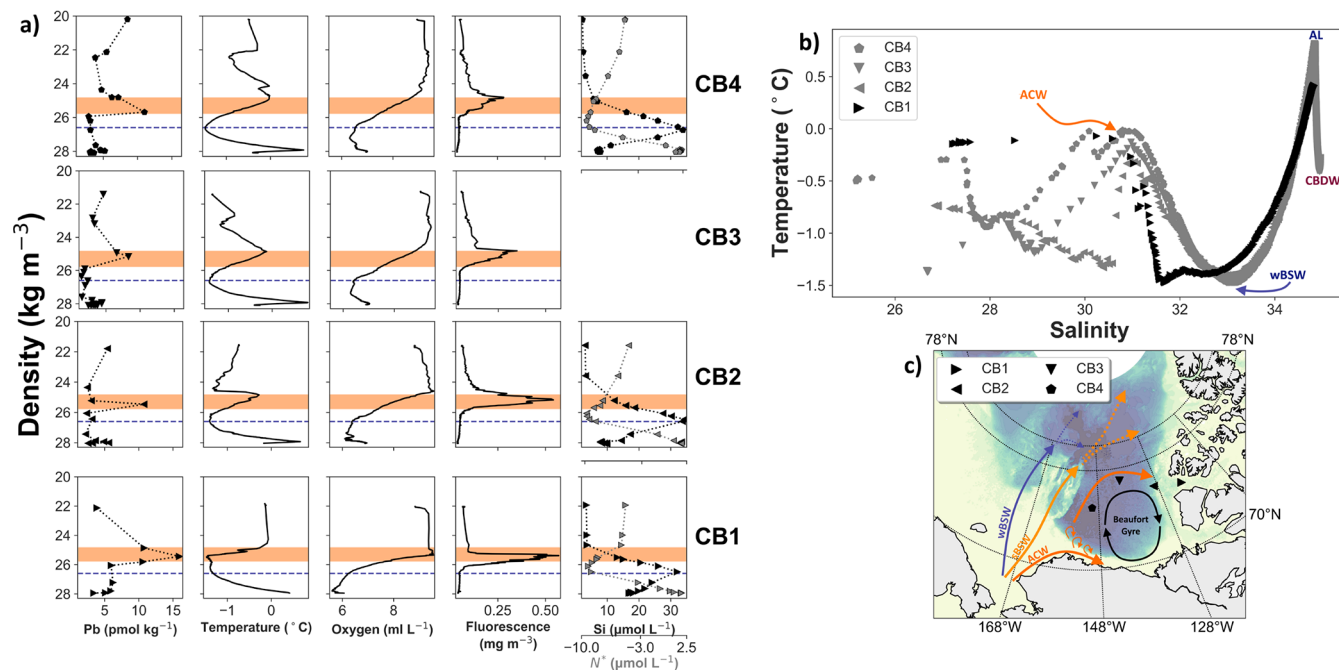


**Figure 3.** (a) Potential density ( $\sigma_\theta$ ) vs Pb, potential temperature, oxygen, fluorescence, and silicate and  $N^*$  (calculated from the following equation:  $N^* = ([\text{NO}_3^- + \text{NO}_2^- + \text{NH}_4^+] - 16[\text{PO}_4^{3-}] + 2.9] \times 0.87$ ; Gruber and Sarmiento<sup>71</sup>). Orange shaded bands indicate the isopycnal surface where Pb peaks ( $\sigma_\theta$ , 24.8–25.8) and the purple dashed line indicates the winter Bering Sea water (wBSW). Silicate and  $N^*$  data from the Canadian GEOTRACES cruise were provided by ArcticNet (Tremblay's group). For those Pb samples for which replicate analyses are available, the error bars reflecting the standard deviation are smaller than the symbols. (b) Potential temperature ( $\theta$ ) vs salinity ( $S$ ) diagram. Gray profiles represent type II waters and black profile type III waters (for details refer to text). ACW, Alaskan coastal water; sBSW, summer Bering Sea water; AL, Atlantic layer; CBDW, Canada Basin deep water. (c) Stations sampled, bathymetry, and schematic of Pacific-derived water circulation in the Canada Basin (after Timmermans et al.<sup>31</sup> and Kondo et al.<sup>44</sup>).

representing only  $3.0 \pm 1.2\%$  of sample cps. Results from the analysis of SAFe D1 ( $25.2 \pm 0.9 \text{ pmol kg}^{-1}$ ;  $n = 5$ ) and GSP ( $63.0 \pm 5.7 \text{ pmol kg}^{-1}$ ;  $n = 5$ ) GEOTRACES reference material were in the range of the reported values by the oceanographic community<sup>19</sup> ( $27.7 \pm 2.6$  and  $62.3 \pm 4.8 \text{ pmol kg}^{-1}$ , respectively; GSP data, Jim Moffett personal communication, GEOTRACES standard and reference trace metal coordinator). The relative standard deviation (1RSD) of SAFe D1 and GSP analysis yield precisions of 3.8 and 9.1% and the RSDs of replicate analysis of control spikes ( $n = 40$ ) were 4% or better. Additionally, the intercalibration exercises carried out with colleagues from numerous universities were in close agreement (Figure S1). The statistical analysis and graphics in this work were developed using Python 3.6.0.

**Ariane Particle Track Simulations.** The sources and paths of the water measured at the stations in Baffin Bay were traced backward from Aug. 8, 2015 to Jan. 1, 2011 using Ariane<sup>51</sup> with five day averaged velocity fields from a 1/12 degree coupled ocean-ice model of the Arctic and Northern Hemispheric Atlantic,<sup>52</sup> based on the Nucleus for European Modeling of the Ocean (NEMO<sup>53</sup>). The model is forced by hourly atmospheric data from the Canadian Meteorological Centre's global deterministic prediction system,<sup>54</sup> Global Ocean Reanalyses and Simulations data for the boundary conditions,<sup>55</sup> and with monthly river runoff climatology.<sup>56</sup> Water parcels at the eight grid points surrounding each station were also tracked to assess their spatial sensitivity and the distributions in resulting paths. On the basis of runs from Aug. 8, 2014 to Jan. 1, 2010 and from Aug. 8, 2016 to Jan. 1, 2012, there is little interannual variability in the tracks.

## RESULTS AND DISCUSSION

This study reports some of the first observations of dissolved Pb concentrations in the Labrador Sea, Baffin Bay, the Canadian Arctic Archipelago, and the Canada Basin. The full data set is presented in Table S2, including those samples that are suspected of contamination, which are flagged in the table and excluded from the discussions below.

In general, low surface concentrations were measured, suggesting that atmospheric inputs are not a main source of Pb in the Canadian Arctic, especially in summer when Arctic aerosol concentrations are at their minimum.<sup>57</sup> Dissolved Pb in the Canada Basin, especially in wBSW and Canada Basin deep water, and in the Canadian Arctic Archipelago were among the lowest reported concentrations in ocean waters,<sup>58</sup> contrasting with the elevated values commonly found in the North Atlantic and the Northwest Pacific Oceans.<sup>27,58</sup> We observed a clear increase in dissolved Pb from the Canada Basin toward Baffin Bay and the Labrador Sea, as well as distinctive advective features of high Pb (Figure 2). We first discuss the Pb distributions in the Canada Basin followed by Baffin Bay and the Labrador Sea. The Pb geochemistry in the Canadian Arctic Archipelago is discussed last, since this region is influenced by the Canada Basin and Baffin Bay end-members.

**Dissolved Lead in the Canada Basin: Influence of Shelf Interactions and Freshwater Inputs. Sea Ice Melt Contributions to the Polar Mixed Layer.** The lowest concentrations ( $4.6 \pm 0.6 \text{ pmol kg}^{-1}$ ) of Pb in surface waters measured during the cruise were in the Canada Basin polar mixed layer (PML) and at some of the stations in the Canadian Arctic Archipelago (CAA2 and CAA7–CAA9). At CB4, however, the PML had almost double ( $8.5 \text{ pmol kg}^{-1}$ )

the surface concentrations measured at CB1–CB3, Figure 3a. The PML at CB4 also yielded the lowest surface salinity ( $S$ , 25.2), compared to the other stations ( $S$ , 26.7–27.6), which reveals the Beaufort Gyre influence on the distribution and storage of freshwater at this station.<sup>59,60</sup> Surface waters in the Canada Basin contain significant amounts of meteoric water, dominated by Eurasian runoff, except in the southern Beaufort Sea where low surface salinities are the result of the entrainment of North American river runoff which does not extend far beyond the shelf break.<sup>61,62</sup> Eurasian and North American Arctic rivers have high Pb concentrations (~50–500 pM<sup>63</sup>); nevertheless, this high signature is removed from the dissolved phase along the salinity gradient due to complex estuarine processes such as particulate settling, flocculation of organomineral complexes and scavenging.<sup>64–66</sup> Therefore, offshore transport of continental runoff is not considered the primary source of the relatively high Pb found in the PML at CB4. In addition to meteoric water, sea ice meltwater represents an important fraction of surface waters (~5–20%), especially in southern Canada Basin where the Beaufort Gyre accumulates freshwater and sea ice.<sup>59,61,62,67</sup> The stations in the Canada Basin were sampled in September, when the release of fresh water from sea ice peaks.<sup>59,62</sup> A water mass analysis performed in this region (Alexis Beaupré-Laperrière, personal communication, following methods similar to Lansard et al.<sup>62</sup>) reveals a higher contribution of sea ice meltwater to surface waters at CB4 (20%) compared with CB1–CB3 (~5–10%), whereas the contribution of meteoric water at CB4 was 7%. The release of trace metals during sea ice melting has been previously suggested as an important mechanism that supplies trace elements to the surface waters.<sup>47,68,69</sup> Recently, dissolved Pb concentrations as high as 33 pM have been measured in Arctic sea ice melt ponds sampled in the Makarov and Canada Basins,<sup>70</sup> indicating that sea ice meltwater may be a plausible source of the higher Pb in the PML at CB4.

**Influence of Pacific-Derived Waters on the Lead Signature in the Canada Basin.** Below the PML, Pb concentrations remained low (2.5–5.5 pmol kg<sup>-1</sup>) down to about 40 m, where the local temperature minimum and an increase in salinity mark the remnant winter mixed layer.<sup>60</sup> The concentrations progressively increased, reaching the highest values measured in the Canada Basin (8.3–15.9 pmol kg<sup>-1</sup>), with a marked shoaling of the peak from CB4 to CB1 (~100 to 40 m) due to the deepening of isopycnal surfaces in the central Beaufort Gyre, Figure 2. Interestingly, when dissolved concentrations are plotted against density, the peak is aligned in a narrow layer at  $\sigma_\theta$  between 24.8 and 25.8 isopycnal surfaces (Figure 3a), and its top ( $\sigma_\theta$ , 24.8) coincides with the temperature maximum of the ACW (upper halocline layer) transitioning to the wBSW (middle halocline layer) by its bottom ( $\sigma_\theta$ , 25.8). This high-Pb feature extends as far as the western region of the Canadian Arctic Archipelago (CAA8), Figure 2. In the same density range, the fluorescence peak lies just below the ACW and at the top of the Si, phosphate, and nitrate nutricline, where solar irradiation and nutrient availability trigger primary production in subsurface waters.<sup>30,72</sup>

Following McLaughlin et al.,<sup>32</sup> two different water mass structures were distinguished from the potential temperature ( $\theta$ ) vs salinity ( $S$ ) plots (Figure 3b). First, the type II waters (CB2–CB4), characterized by a distinct temperature maximum (>−1.0 °C) in the upper halocline (ACW) with salinity profiles displaying large regional variability in the top 300 m

(29 <  $S$  ≤ 32.2). The Pb concentrations in or just below the ACW water from CB2 to CB4 had similar values (10.0 ± 1.2 pmol kg<sup>-1</sup>). Slightly higher Pb concentrations (15.9 pmol kg<sup>-1</sup>) were measured in the type III waters at CB1 west of Banks Island; these waters are distinguished by a warm surface halocline in the range 27 <  $S$  < 31.5, probably developed by solar heating of ice-free surface waters. Below  $S$  = 31.5, the  $\theta$ – $S$  shapes of wBSW and lower halocline water were distinct from those of the central Canada Basin.<sup>31,32</sup>

The ACW occupies most of the Beaufort Sea and the North American continental slope, and regardless of the water type, high Pb was observed at the four stations. This high-Pb signature can be traced from the northeast Subarctic Pacific (GEOTRACES cruise GP02), where concentrations in the upper 200 m range from approximately 40 to 50 pmol kg<sup>-1</sup>,<sup>22</sup> as a result of the increased industrial emissions from Asian countries and Russia over the past 4 decades.<sup>27</sup> During its transit through the Bering and Chukchi Seas, this high-Pb signal is weakened, with concentration ranging from 13 to 20 pmol kg<sup>-1</sup> on the Bering Sea slope and from 3 to 13 pmol kg<sup>-1</sup> in Bering Strait (Robert Rember personal communication; 2015 U.S. GEOTRACES Arctic cruise GN01), values that are in the same range as those observed in the ACW across the Canada Basin. The decrease of this high signature from the Northeast Subarctic Pacific to the Canada Basin is attributed primarily to the efficient scavenging of Pb, a highly particle reactive element, in the shallow and productive Bering and Chukchi shelves,<sup>37,73</sup> yielding short residence times in this region (<1 year).<sup>70,74,75</sup>

**Enhanced Lead Removal in Near-Bottom Winter Bering Sea Water.** Beneath the upper halocline Pb peak, low concentrations were found across the wBSW and Atlantic-derived lower halocline layer (~100–300 m), with lower concentrations at stations CB2–CB4 (type II waters) than at CB1, type III water (2.2 ± 0.7 vs 6.0 ± 0.1 pmol kg<sup>-1</sup>). Although ACW and wBSW are both of Pacific origin, they exhibit distinctive physicochemical properties, aside from those observed for Pb. Compared with ACW, wBSW is distinguished by a weak temperature minimum near  $S$  = 33.1, high nutrient concentrations, nutrient-like trace metals, high dissolved organic matter, and low oxygen concentrations,<sup>44,76</sup> Figure 3a.

These distinctive properties provide evidence that wBSW undergoes notable organic matter remineralization in the Bering and Chukchi shelves.<sup>76,77</sup> In summer the surface waters are freshened by sea ice melt, isolating wBSW to a deeper layer in close proximity with the sediment. Nutrients are rapidly drawn down from surface waters due to summer phytoplankton blooms, increasing the particle flux, and prompting organic matter remineralization and oxygen consumption in the underlying wBSW.<sup>77</sup> Dissolved Pb distributions, unlike nutrient-like trace metals, are low in the cold, near-bottom wBSW, revealing a potential enhanced removal of Pb at the sediment–water boundary by sediment resuspension events over the extensive continental shelves.<sup>74,75,78</sup> The negative  $N^*$  values of wBSW (Figure 3a) indicate that this water was influenced by sedimentary denitrification and/or anammox in the Bering and Chukchi shelves.<sup>44,76,77,79</sup> Under reducing sediment conditions, which trigger the nitrogen benthic loss, an increase of Mn and Fe in near-bottom waters has been observed in the Chukchi Sea.<sup>79</sup> These redox sensitive elements are mobilized from the sediments, diffusing into the bottom water where they become oxidized and precipitate back to the sediments.<sup>79</sup> In this context Pb can be further removed from

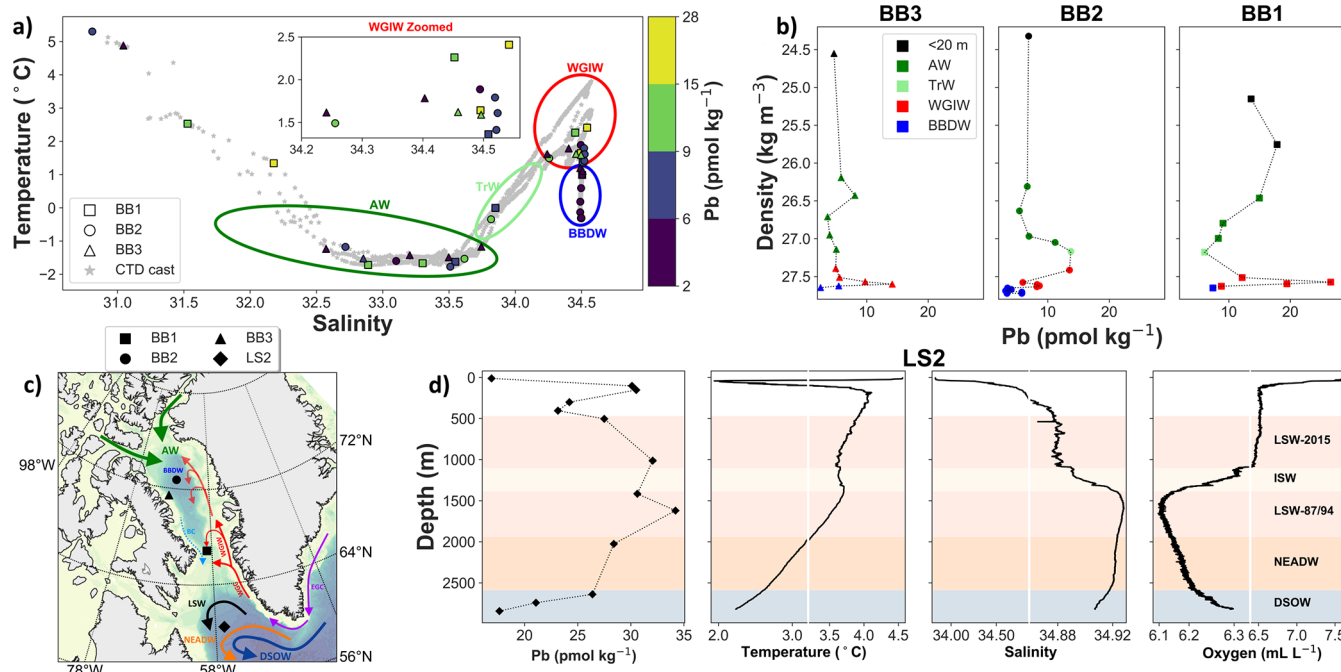


**Figure 4.** (a) Potential temperature ( $\theta$ ) vs salinity ( $S$ ) diagram from Baffin Bay stations with Pb concentrations for the analyzed samples (color scale). Water masses in Baffin Bay were identified following Tang et al.<sup>40</sup> and Curry et al.<sup>46</sup> WGIW, West Greenland intermediate water; TrW, transitional water; AW, Arctic water; BBDW, Baffin Bay deep water. (b) Potential density ( $\sigma_\theta$ ) vs dissolved Pb in Baffin Bay. (c) Sampled stations, bathymetry, and schematic circulation (after Yashayaev and Clarke,<sup>45</sup> Curry et al.,<sup>46</sup> and Lozier et al.<sup>42</sup>) in Baffin Bay and the Labrador Sea. EGC, East Greenland current; WGC, West Greenland current; BC: Baffin current; LSW, Labrador Sea water; ISW, Icelandic Slope water; NEADW, Northeast Atlantic deep water; DSOW, Denmark Strait overflow water. (d) Dissolved Pb,  $\theta$ , S, and oxygen profiles in the Labrador Sea. The water masses were identified following Yashayaev and Loder.<sup>41,84</sup> For those Pb samples for which replicate analyses are available, the error bars reflecting the standard deviation are smaller than the symbols.

the dissolved phase in near-bottom waters during the Mn redox cycle either by its coprecipitation with Mn oxides or the adsorption onto Mn oxides coated particles,<sup>80</sup> a phenomena which is anticipated to co-occur with the precipitation of Fe oxides under the same circumstances.

**Lead Distributions in Atlantic and Canada Basin Deep Waters.** A slight increase in Pb ( $4.6 \pm 0.8 \text{ pmol kg}^{-1}$ ) is observed in the warm Atlantic layer (~300 to 800 m;  $\sigma_\theta = 27.9$ ), reflecting the circulation of the Fram Strait Branch (FSB) in the boundary current along the continental slope, Figures 2 and 3a. Lead has a short residence time (20–80 years) in thermocline and deep waters.<sup>13,15</sup> As a result, the Pb signature of the FSB, advected from the Norwegian Sea, has undergone significant scavenging and mixing with surrounding waters during its flow from Fram Strait to Canada Basin (20–50 years<sup>81</sup>), and thus its initial high-Pb signature has almost vanished. Underlying the Atlantic layer, low concentrations ( $3.2 \pm 0.3 \text{ pmol kg}^{-1}$ ) were measured in Canada Basin deep waters (1500–3500 m). In addition to scavenging removal of Pb, this old (~500 years) and isolated water mass<sup>81,82</sup> was ventilated before the peak in anthropogenic Pb emissions, yielding a preanthropogenic low signature.

**Tracing the Far-Reaching Footprint of Lead in the Labrador Sea and Baffin Bay.** A common feature in Baffin Bay is the low concentration of Pb found in the surface mixed layer (~11.5 m), with lower values measured at the central stations (BB2 and BB3) than at the southern BB1 ( $5.8 \pm 1.1$  vs  $13.6 \text{ pmol kg}^{-1}$ ), Figure 4b,c. Underneath the mixed layer, four water masses can be identified by their temperature and salinity properties: The West Greenland intermediate water (WGIW) of North Atlantic origin, the Arctic water (AW)

produced by winter convection and mixing between WGC and Arctic-derived waters, the transitional water (TrW) laying between AW and WGIW, and the Baffin Bay deep water,<sup>46,83</sup> Figure 4a. The concentrations of Pb in the AW, characterized as subzero water with a salinity range of 32.0–33.7, were relatively low at BB2 and BB3 ( $6.3 \pm 0.7$  and  $5.3 \pm 1.5 \text{ pmol kg}^{-1}$ ) and slightly higher at BB1 ( $10.8 \pm 3.0 \text{ pmol kg}^{-1}$ ). Underlying AW and TrW, lies the WGIW (~300–800 m) distinguished by its warm temperature ( $\theta > 1.3$ ) and high salinity ( $S \geq 34.2$ ). The highest Pb concentrations were found in the narrow WGIW isopycnal range ( $\sigma_\theta$ , 27.4–27.6), representing the densest water that crosses the Davis Strait sill from the Labrador Sea, Figure 4b. As was noted for Pb concentrations in the mixed layer and AW, the Pb peak in the WGIW at BB2 and BB3 was lower than at BB1 (13.5 and 14.1 vs  $26.6 \text{ pmol kg}^{-1}$ , respectively). The higher Pb at BB1, located in the central part of Davis Strait, is associated with the first recirculation of the northward WGC inflow which has uniformly high Pb concentration ( $23.6 \pm 1.0 \text{ pmol kg}^{-1}$ ) in the upper 1000 m at the western tip of the Greenland slope.<sup>23</sup> These high values are attributed to the Irminger Sea water (ISW), a remnant of the North Atlantic current spreading northwestward along the Reykjanes Ridge, circulating cyclonically in the Irminger and Labrador Seas and advecting warm, salty, and anthropogenically elevated Pb waters.<sup>18,19,23,42,83</sup> The subsurface layers of the WGC are mixed with neighboring cold, fresh, and low-Pb waters advected from the Arctic Ocean, leading to the cooling, freshening, and weakening of the Atlantic Pb signature in AW and TrW in western Baffin Bay, especially at BB3. Nonetheless, this mixing is small in the warmer and saltier WGIW core, where high Pb was found in all

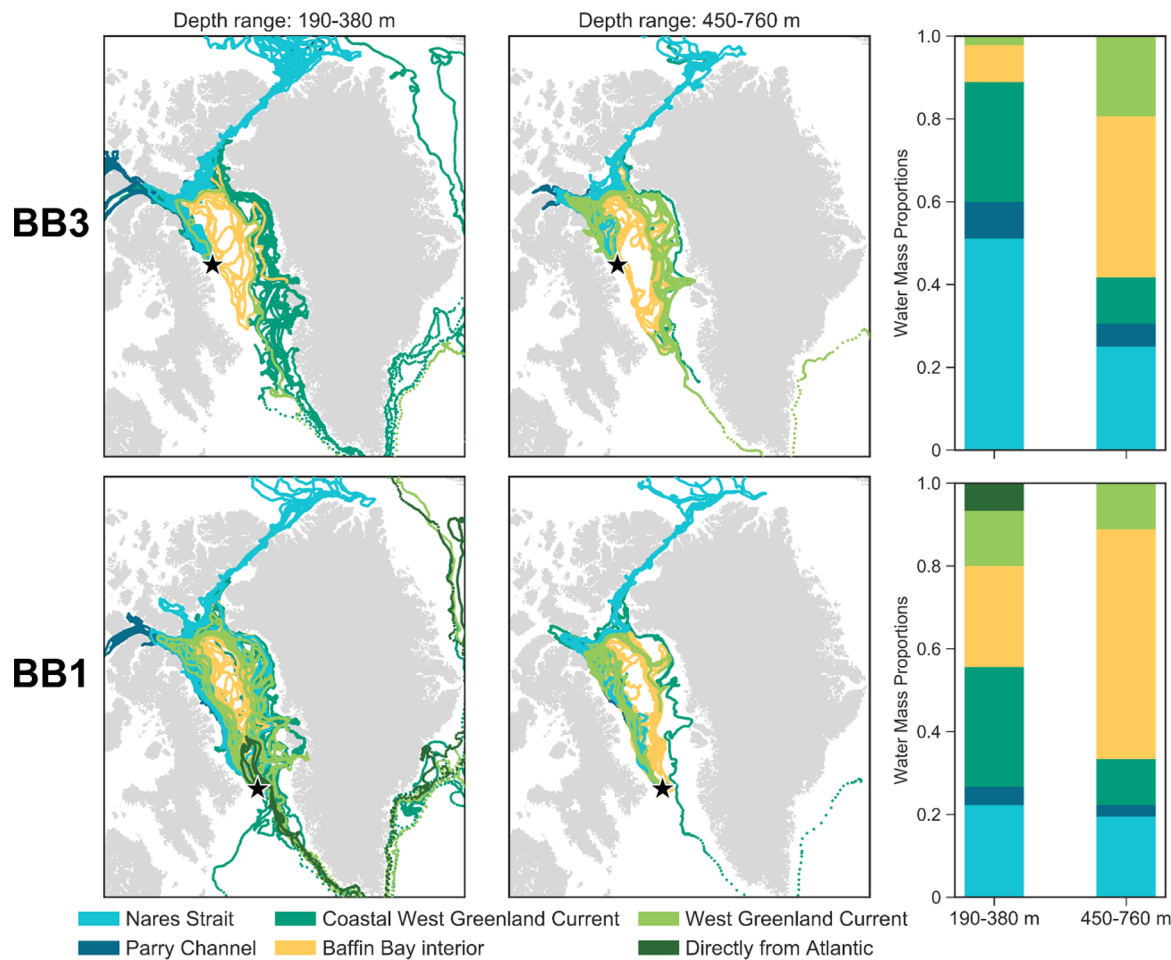


**Figure 5.** Water mass back-trajectories from station BB3 (upper panel) and BB1 (lower panel) from 2015 back to 2011 over two depth ranges. Tracks were grouped according to their origin and path; this breakdown is shown in proportions in the bar plots on the right. The groups are as follows: Nares Strait, originates from the Arctic Ocean and passes through Nares Strait; Parry Chanel, originates from the Arctic Ocean and passes through Perry Chanel; coastal West Greenland current, originates from the WGC and travels into the CAA, where it mixes with Arctic waters; Baffin Bay interior, circulates in the Baffin Bay interior for the entire time period; West Greenland current, travels from the Atlantic via the WGC around Baffin Bay; directly from Atlantic, travels directly from the Atlantic to the station without circulating around Baffin Bay.

Baffin Bay stations, Figure 4b. The relatively high concentrations ( $12.9 \pm 1.2 \text{ pmol kg}^{-1}$ ) in TrW ( $\sim 150\text{--}200 \text{ m}$ ) at BB2 are comparable to those observed in WGIW at BB2 and BB3 (13.5 and  $14.1 \text{ pmol kg}^{-1}$ , respectively) and illustrate the shallow mixing of the WGC with Arctic-derived waters in central Baffin Bay. In the eastern and central region of Baffin Bay the AW extends to a depth of approximately 100 m, progressively deepening during its cyclonic circulation due to the inflow of fresher waters from the Arctic Ocean in the northwest region of the bay.<sup>40</sup>

In order to assist with the interpretation of Pb distributions in Baffin Bay, water mass back-trajectories were calculated from ANHA12 simulations. This analysis supports our interpretations above, showing that surface waters ( $<450 \text{ m}$ ) are greatly influenced by Arctic-derived waters, while, below  $\sim 450 \text{ m}$ , waters tend to originate from the Baffin Bay interior and WGC. Additionally, the trajectories illustrate the augmented Arctic outflow at station BB3, where, from approximately 190 to 400 m, the waters are directly exported from the Arctic Ocean to Baffin Bay through Parry Chanel and Nares Strait ( $\sim 60\%$  of surface water), and the water advected by the WGC travels into Smith and Lancaster Sounds, likely mixing with Arctic waters with lower Pb concentrations ( $\sim 20\%$

of surface water), Figures 5 and S2. The trajectories also show that the addition of Arctic waters at BB3 is mostly restricted to the upper 400 m; below this depth, water masses that have not been significantly mixed with Arctic-derived waters, such as from the WGC and Baffin Bay interior, are prevalent ( $\sim 60\%$ ). This coincides with the depths where the high-Pb feature is observed (Figures 3b and 4). A similar pattern is observed at BB1, although the surface waters ( $<450 \text{ m}$ ) receive an augmented contribution from the Baffin Bay interior and some water is directly advected from the Labrador Sea, likely explaining the relatively high-Pb values measured at BB1 compared with the central Baffin Bay stations (Figures 4b, 5, and S2).

The Baffin Bay Deep Water (BBDW;  $>1200 \text{ m}$ ) is characterized by a small change in salinity and a constant decrease in potential temperature (Figure 4a); this deep and old water has no direct access to the Arctic and Atlantic Oceans, and its origin is under discussion.<sup>40</sup> The BBDW had the lowest Pb concentration measured in Baffin Bay ( $2.5\text{--}7.4 \text{ pmol kg}^{-1}$ ), attributed to the ventilation age of this old water, presumably before times of higher anthropogenic Pb deposition, and the scavenging throughout the deep water column.

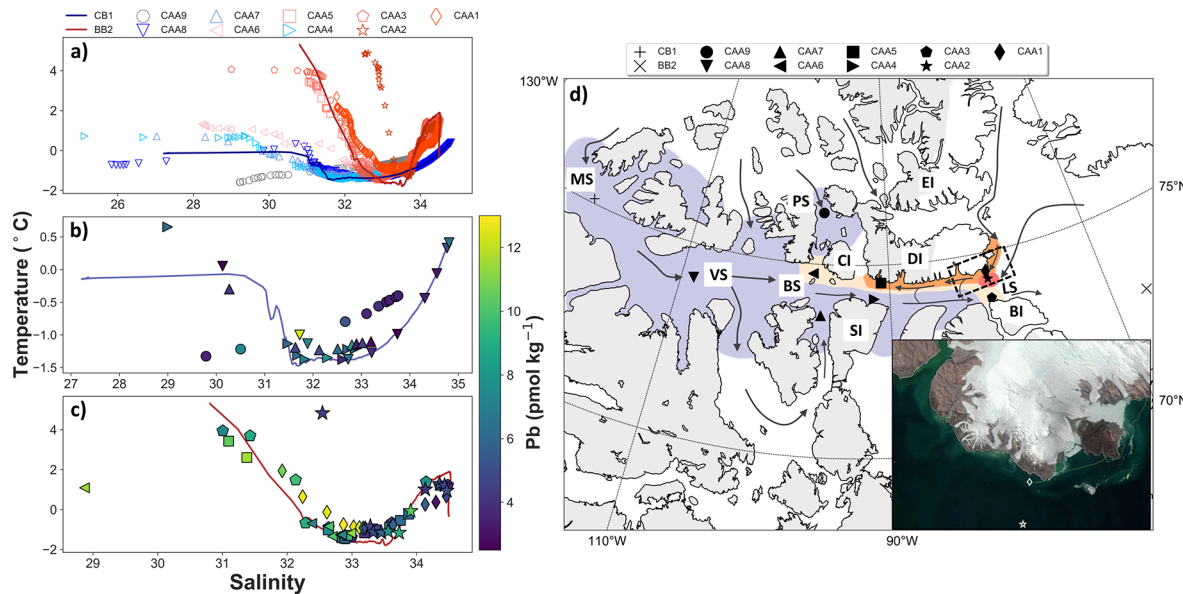


**Figure 6.** (a) CTD temperature ( $\theta$ ) vs salinity ( $S$ ) diagram for all the stations in the CAA. Those stations influenced by Baffin waters (Atlantic signature) are displayed with red colors, while the stations influenced by Arctic waters are displayed with blue colors. The  $\theta/S$  data from the Canada Basin end-member (CB1) and Baffin Bay end-member (BB2) are shown with blue and red solid lines, respectively. (b) Pb concentration (color scale),  $\theta$ , and  $S$  data measured at CAA7–CAA9 and CAA4. (c) Pb concentration (color scale),  $\theta$ , and  $S$  data measured at CAA7–CAA9 and CAA4. Note that temperature/salinity axes vary between plots. (d) Sampled stations and conceptual scheme of water masses and circulation pathways in the CAA (after Michel et al.,<sup>34</sup> and Wang et al.<sup>36</sup>). The inset includes a Terra-MODIS visible image of eastern Devon Island taken on Jul. 25, 2015 (<https://worldview.earthdata.nasa.gov/>), illustrating the presence of glacial runoff along the Devon Island coast. Light blue, Arctic-derived waters (low Pb); red, Atlantic-derived water (high Pb); orange, glacially modified surface waters (high-Pb surface waters); light orange, mixing between glacial runoff, Atlantic and Arctic waters. MS, M'Clure Strait; VS, Viscount Melville Sound; BS, Barrow Strait; PS, Penny Strait; LS, Lancaster Sound; CI, Cornwallis Island; SI, Somerset Island; DI, Devon Island; BI, Bylot Island; EI, Ellesmere Island. Parry Channel is the main pathway in central CAA connecting M'Clure Strait with Lancaster Sound.

The surface concentration in the Labrador Sea ( $16.9 \text{ pmol kg}^{-1}$ ) agrees with that reported by Zurbrick et al.<sup>23</sup> during the 2014 GEOVIDE cruise ( $12.1\text{--}16.2 \text{ pmol kg}^{-1}$ ). This concentration is higher than the levels found in central Baffin Bay ( $5.8 \pm 1.1 \text{ pmol kg}^{-1}$ ) but similar to those found in Davis Strait ( $13.6 \text{ pmol kg}^{-1}$ ), supporting the recirculation of the WGC observed at BB1. A sharp increase in Pb ( $30.5 \pm 0.3 \text{ pmol kg}^{-1}$ ) is observed below the mixed layer around 100 m, as a result of the advection of modified ISW carried by WGIW from Baffin Bay, where comparable concentrations ( $26.6 \text{ pmol kg}^{-1}$ ) were measured at Davis Strait in a similar density range ( $\sigma_\theta$ ,  $27.5\text{--}27.6$ ), Figure 4d.

In the deep water column ( $\sim 500\text{--}2500 \text{ m}$ ), Pb was high ( $26.4\text{--}34.2 \text{ pmol kg}^{-1}$ ) and uniformly distributed across multiple hydrographic features (Figure 4d), as observed by Zurbrick et al.<sup>23</sup> In 2015, when the Canadian Arctic GEOTRACES cruise took place, two LSW classes were clearly distinguished by the conductivity–temperature–depth (CTD) observations: the newly ventilated and fresher LSW formed during the winters of 2014 and 2015 (LSW-2015) and the old, saltiest, and least oxygenated LSW produced in the winters of 1987–1994 (LSW-87/94), which was the densest and most voluminous LSW class formed in recent years.<sup>41</sup> The thin, relatively saline and warm layer that lies between the two LSW classes is the Icelandic Slope water.<sup>84,85</sup> Underlying the LSW-87/94 lies the saline, warm ( $\theta \sim 3 \text{ }^\circ\text{C}$ ;  $S \sim 34.92$ ) and less oxygenated Northeast Atlantic deep water (NEADW). The deepest water is the less saline, colder ( $\theta \leq 2.6 \text{ }^\circ\text{C}$ ;  $S \sim 34.9$ ), and more recently oxygenated Denmark Strait overflow water,<sup>41,43,86</sup> Figure 4d. Numerous processes are likely to account for the Pb maximum spreading across the LSW-2015,

LSW-87/94, and NEADW. Among them, the deep convection taking place in 2015 mixing the ISW with older LSW formed during previous years,<sup>41,84,85</sup> scavenging removal of Pb in the old LSW-87/94 waters, with approximately 45% reduction between the concentrations measured in the LSW in 1993 during the IOC II cruise<sup>18</sup> and those measured in the residual LSW-87/94 in 2015, and the advection of NEADW from the Norwegian Sea are the most significant processes modulating Pb distributions below  $\sim 500 \text{ m}$ .

The Pb concentration dropped from the NEADW to the deep Denmark Strait overflow water (DSOW) reaching  $17.6 \text{ pmol kg}^{-1}$  at  $\sim 2800 \text{ m}$ . During deep convection, surface and subsurface waters are subducted, entraining the Pb signature to the deep ocean. Therefore, differences in the ventilation time and place between these two water masses may explain the disparity in Pb distributions. Even though the DSOW was ventilated more recently than the NEADW (5–8 vs 11–13 years<sup>87</sup>), DSOW Pb concentrations have remained relatively low ( $< 20 \text{ pmol kg}^{-1}$ ) during the past 20 years,<sup>18</sup> indicating that the ventilation time is not the main driver of Pb concentrations in DSOW. The NEADW and DSOW originate in different regions; DSOW is produced in the Greenland Sea, receiving the fresh and low-Pb Arctic outflow,<sup>42,84</sup> whereas NEADW is the result of dense overflow waters produced in the Norwegian Sea, where the Iceland Scotland overflow water evolves into the NEADW. The Norwegian Sea is influenced by the North Atlantic current bringing warm and high-Pb upper-ocean waters from the subtropical western North Atlantic.<sup>19,21</sup> As observed for Pb, the concentrations of dissolved  $^{230}\text{Th}$ , a highly particle reactive radionuclide, decreased below  $\sim 2500 \text{ m}$  in DSOW at LS2,<sup>88</sup> suggesting that enhanced bottom scavenging

of Pb by sediment resuspension could be an additional process affecting Pb distribution in DSOW. Similarly, in the North Atlantic, from Massachusetts to the Bermuda Atlantic Time Series station, the depletion of  $^{230}\text{Th}$  in DSOW was associated with bottom scavenging throughout the thick nepheloid layer, where a concomitant decrease in dissolved Pb was observed.<sup>19,89</sup>

**Lead Distributions in the Dynamic Canadian Arctic Archipelago.** Two main domains are recognized in the Canadian Arctic Archipelago based on CTD and Pb data. Arctic waters of Pacific origin, entering through M'Clure and Penny Straits, travel predominantly along the southern side of Parry Channel (CAA7–CAA9 and CAA4). These waters are cooler ( $-1.6\text{ }^{\circ}\text{C} < \theta < 0.8\text{ }^{\circ}\text{C}$ ) and fresher ( $25.1 < S < 34.8$ ) compared to Baffin waters of Atlantic origin recirculating in the eastern CAA ( $-1.5\text{ }^{\circ}\text{C} < \theta < 4.9\text{ }^{\circ}\text{C}; 28.2 < S < 34.5$ ). Likewise, Pb has distinctive distributions and lower concentrations in the stations influenced by the Arctic outflow, relative to those influenced by Atlantic waters (Figures 6a,b,c and S2).

The vertical Pb distribution in Viscount Melville Sound (CAA8) resembles that of CB1, with low concentrations in the PML ( $1.7\text{ pmol kg}^{-1}$ ) and a sharp increase between 40 and 100 m ( $6.4\text{--}12.5\text{ pmol kg}^{-1}$ ) linked to the advection of the upper halocline layer ( $\sigma_{\theta} 24.8\text{--}25.8$ ) from Canada Basin, Figure 2. The middle and lower halocline waters (100–300 m; Pb,  $3.5 \pm 0.8\text{ pmol kg}^{-1}$ ) as well as the Atlantic waters ( $>300\text{ m}; 5.7 \pm 0.7\text{ pmol kg}^{-1}$ ) are transported from Canada Basin along the western Parry Channel, one of the deepest regions ( $\sim 500\text{ m}$ ) of the archipelago, as far as Viscount Melville Sound. Only the surface and Pacific-derived waters (ACW and wBSW) are able to cross the shallow Barrow Strait, and their properties are modified throughout the eastward journey to Baffin Bay. The Pb distribution in Barrow Strait (CAA7) and north of Somerset Island (CAA4) were consistent with those found in Canada Basin, showing low concentrations in the upper 50 m ( $4.6 \pm 0.4$  and  $6.2 \pm 0.1\text{ pmol kg}^{-1}$ , respectively), a maximum between  $\sim 60$  and 100 m ( $7.3 \pm 0.9\text{ pmol kg}^{-1}$ ), and returning to lower values below 100 m ( $3.3 \pm 0.7$  and  $5.2 \pm 0.8\text{ pmol kg}^{-1}$ , respectively). The slightly higher concentrations found at CAA4 may indicate the recirculation of Baffin waters traveling westward along the northern side of Parry Channel (discussed below). The station in Penny Strait (CAA9) captures the southward flow from the Arctic Ocean to the CAA interior; the near linearity of the  $\theta$ –S profile (Figure 6b) is consistent with the strong tidal mixing in this region. Despite the fact that Canada Basin  $\theta$ –S features have faded, the relatively low Pb concentrations measured in Penny Strait ( $3.2\text{--}7.4\text{ pmol kg}^{-1}$ ) indicate the prevailing Arctic origin of these waters.

Baffin waters enter the CAA through Lancaster Sound, traveling westward along the northern side of Parry Channel, joining the Arctic outflow waters near Barrow Strait, and exiting the archipelago on the southern side of Lancaster Sound,<sup>36</sup> Figure 6d. On the northern side of Lancaster Sound, an unanticipated difference in most of the physicochemical properties and Pb concentrations was observed between CAA1 and CAA2, especially in the upper 60 m. Although these two stations are  $\sim 20\text{ km}$  apart from each other, surface waters at CAA1 were noticeably fresher ( $31.8\text{--}32.9$  vs  $32.5\text{--}33.4$ ) and cooler ( $-0.7\text{--}2.7$  vs  $-1.2\text{--}4.9\text{ }^{\circ}\text{C}$ ) than those at CAA2, Figure 6c. Similarly, Pb concentrations in the surface were significantly ( $P < 0.05$ ) higher at CAA1 than at CAA2 ( $12.4$

$\pm 1.0$  vs  $4.8 \pm 0.5\text{ pmol kg}^{-1}$ ). The aforementioned discrepancies suggest that an additional freshwater source is present along the Devon Island coast near CAA1. The CAA has one of the largest volumes of glacier ice on Earth with approximately 10% of its surface covered by glaciers, which are mainly distributed along the western sides of Ellesmere, Devon, and Baffin islands, and on Bylot Island.<sup>92</sup> Station CAA1 was located in close proximity ( $\sim 5\text{ km}$ ) to the Devon coast, receiving the meltwater runoff from Devon glaciers during the summer season, Figure 6d. Sediment-laden meltwater runoff from these glaciers would explain not only the fresher and cooler surface waters at CAA1 but also the decrease in transmissivity measured at CAA1, as observed in subsurface glacial plumes ( $\sigma_{\theta} 25.0\text{--}26.5$ ) in Greenland fjords close to northern Baffin Bay.<sup>93</sup> Concentrations of dissolved Pb in glacial streams from CAA are  $\sim 6$  to 50 times greater (35 pM) than those found in other central CAA rivers.<sup>63</sup> Hence, the mixing of glacial runoff with Baffin waters could explain the high Pb observed in the subsurface plume ( $\sigma_{\theta} 25.5\text{--}26.6$ ) traveling along Devon Island (CAA1 and CAA5). Below this plume, concentrations dropped ( $5.3 \pm 1.1\text{ pmol kg}^{-1}$ ) from 120 m until the bottom, Figure S3. From the  $\theta$ –S diagram it can be seen that waters at CAA2 do not contain glacial runoff waters. The distinctive physical properties and Pb signature from Baffin waters are preserved, with low surface concentrations ( $4.8 \pm 0.5\text{ pmol kg}^{-1}$ ), peaking in TrW from 80 to 150 m ( $\sigma_{\theta} 26.9\text{--}27.2; 9.1 \pm 1.0\text{ pmol kg}^{-1}$ ), as observed at BB2, and returning to lower values below 200 m ( $4.8 \pm 0.4\text{ pmol kg}^{-1}$ ), Figure S6c and S3.

Finally, CAA3 and -6 represent transition stations influenced by multiple water sources such as Arctic-derived waters, Baffin Bay waters, and glacial inputs. CAA3 station, located in southern Lancaster Sound (Bylot Island coast), receives the Arctic outflow flowing along southern Parry Channel, Baffin Bay waters recirculating in eastern Parry Channel, and glacial inputs (Figure 6d). The concentrations in the upper 50 m at CAA3 were higher ( $8.7 \pm 0.9\text{ pmol kg}^{-1}$ ) than those observed in surface waters at CAA4 and CAA7–CAA9, reflecting the mixing of low-Pb Arctic-origin waters with the recirculation of the glacial subsurface plume from Devon Island, albeit local glacial inputs from Bylot Island cannot be excluded. The lower values ( $4.4 \pm 0.8\text{ pmol kg}^{-1}$ ) measured in intermediate waters ( $\sim 60\text{--}200\text{ m}$ ) were comparable to those found in AW in Baffin Bay and Canada Basin waters in western CAA, and the slight Pb increase from  $\sim 200$  to 400 m corresponds to TrW. The CAA6 station, located in Barrow Strait west of Cornwallis Island, receives the remnants of Baffin Bay waters and glacial inputs from Devon Island, as well as Arctic waters flowing southward from Penny Strait and entering through M'Clure Strait (Figure 6d). Despite the Arctic influence, the relatively high-Pb signatures found at CAA1 and CAA5 were still traced at CAA6 ( $7.03\text{--}11.65\text{ pmol kg}^{-1}$ ).

## CONCLUSION

This study presents some of the first observations of dissolved Pb across the Labrador Sea, Baffin Bay, the Canadian Arctic Archipelago, and the Canada Basin which were made during the GEOTRACES Canadian program in 2015. This extensive data set not only provides a baseline for assessing future Pb studies in the Arctic but also will contribute to a better understanding of the global Pb cycle. The Canada Basin and the Canadian Arctic Archipelago are relatively isolated from anthropogenic inputs, with the lowest Pb concentrations (<7

pmol kg<sup>-1</sup>) measured in this study and among the lowest reported in the literature. Nonetheless, remnants of anthropogenic pollution in the form of higher Pb concentrations (~10–25 pmol kg<sup>-1</sup>) were clearly traced in the Canada Basin from the northeast Subarctic Pacific and in Baffin Bay from the North Subarctic Atlantic, overlying the pervasive low concentrations. Lead concentrations in the Labrador Sea yielded the highest concentrations (~17–34 pmol kg<sup>-1</sup>) measured in this study, reflecting the influence of the subpolar gyre circulation advecting warm, salty, and anthropogenically elevated Pb waters. In addition to the anthropogenic influence, the distribution of dissolved Pb in the Canadian Arctic is modulated by natural processes occurring at the continent–ocean interface such as glacial water runoff and sea ice melt (inputs), and at the sediment–water boundary (scavenging–removal–sinks). Finally, we integrate modeling data along with field observations to unravel the Pb distribution in Baffin Bay, demonstrating that dissolved lead is a useful complementary tracer of water masses in the Canadian Arctic Ocean. These new Pb data collected during the GEOTRACES Canadian program, along with Pb isotopes, major nutrients and micronutrients data, will improve our knowledge about the dynamic Arctic ocean environment.

## ■ ASSOCIATED CONTENT

### Supporting Information

The Supporting Information is available free of charge on the ACS Publications website at DOI: [10.1021/acsearthspacechem.9b00083](https://doi.org/10.1021/acsearthspacechem.9b00083).

Figures S1–S3 showing depth profiles, intercalibration exercises, water mass back-trajectories and proportions, and interpolated contours of dissolved Pb and corresponding maps showing sampling stations and Tables S1 and S2 listing sampling stations and dissolved Pb concentrations ([PDF](#))

## ■ AUTHOR INFORMATION

### Corresponding Author

\*E-mail: [mcolombo@eoas.ubc.ca](mailto:mcolombo@eoas.ubc.ca).

### ORCID

Manuel Colombo: [0000-0001-9869-4802](https://orcid.org/0000-0001-9869-4802)

### Notes

The authors declare no competing financial interest.

## ■ ACKNOWLEDGMENTS

This work was supported by the Natural Sciences and Engineering Research Council of Canada (Grant NSERC-CCAR) and the Northern Scientific Training Program. We thank the captain and crew of the CCGS *Amundsen* as well as Chief Scientist Roger Francois and the science crew of the Canadian Arctic GEOTRACES program for their assistance in sample collection. We also thank Alexis Beaupré-Laperrière and Alfonso Mucci's group for providing the water mass analysis of Canada Basin, ArcticNet; Jean-Eric Tremblay's group for providing the nutrient data for the Canadian GEOTRACES 2015 cruise; and Robert Remer for the fruitful conversation about Pb distributions in the Canada Basin and Pb concentration ranges for the Bering and Chukchi Sea. The University of British Columbia PCGIR and its staff are thanked for assistance with sample analyses. We are grateful to the NEMO development team and the Drakkar project for

providing the model and continuous guidance and to Westgrid and Compute Canada for computational resources. We thank three anonymous reviewers for their thoughtful comments, which helped to improve this manuscript.

## ■ REFERENCES

- (1) Nriagu, J. O.; Pacyna, J. M. Quantitative Assessment of Worldwide Contamination of Air, Water and Soils by Trace Metals. *Nature* **1988**, *333* (6169), 134–139.
- (2) Nriagu, J. O. The Rise and Fall of Leaded Gasoline. *Sci. Total Environ.* **1990**, *92* (C), 13–28.
- (3) Callender, E. Heavy Metals in the Environment — Historical Trends. *Treatise on Geochemistry*, 2nd ed.; Reference Module in Earth Systems and Environmental Sciences; Elsevier, 2013; Vol. 11, pp 59–89, [DOI: 10.1016/B978-0-08-095975-7.00903-7](https://doi.org/10.1016/B978-0-08-095975-7.00903-7).
- (4) Mahowald, N. M.; Hamilton, D. S.; Mackey, K. R. M.; Moore, J. K.; Baker, A. R.; Scanza, R. A.; Zhang, Y. Aerosol Trace Metal Leaching and Impacts on Marine Microorganisms. *Nat. Commun.* **2018**, *9* (1), 2614.
- (5) Graney, J. R. J. R.; Halliday, A. N. A. A. N.; Keeler, G. J. G. G. J.; Nriagu, J. O. J. O.; Robbins, J. A. A. J.; Norton, S. A. A. S. A. Isotopic Record of Lead Pollution in Lake Sediments from the Northeastern United States. *Geochim. Cosmochim. Acta* **1995**, *59* (9), 1715–1728.
- (6) Lima, A. L.; Bergquist, B. A.; Boyle, E. A.; Reuer, M. K.; Dudas, F. O.; Reddy, C. M.; Eglington, T. I. High-Resolution Historical Records from Pettaquamscutt River Basin Sediments: 2. Pb Isotopes Reveal a Potential New Stratigraphic Marker. *Geochim. Cosmochim. Acta* **2005**, *69* (7), 1813–1824.
- (7) Cheyne, C. A. L.; Thibodeau, A. M.; Slater, G. F.; Bergquist, B. A. Lead Isotopes as Particulate Contaminant Tracers and Chronostratigraphic Markers in Lake Sediments in Northeastern North America. *Chem. Geol.* **2018**, *477*, 47–57.
- (8) Osterberg, E. C.; Mayewski, P.; Kreutz, K.; Fisher, D.; Handley, M.; Sneed, S.; Zdanowicz, C.; Zheng, J.; Demuth, M.; Waskiewicz, M.; Bourgeois, J. Ice Core Record of Rising Lead Pollution in the North Pacific Atmosphere. *Geophys. Res. Lett.* **2008**, *35* (5), L05810.
- (9) Gross, B. H.; Kreutz, K. J.; Osterberg, E. C.; McConnell, J. R.; Handley, M.; Wake, C. P.; Yalcin, K. Constraining Recent Lead Pollution Sources in the North Pacific Using Ice Core Stable Lead Isotopes. *J. Geophys. Res.: Atmos.* **2012**, *117* (16), D16307.
- (10) Shen, G. T.; Boyle, E. A. Lead in Corals: Reconstruction of Historical Industrial Fluxes to the Surface Ocean. *Earth Planet. Sci. Lett.* **1987**, *82* (3–4), 289–304.
- (11) Kelly, A. E.; Reuer, M. K.; Goodkin, N. F.; Boyle, E. A. Lead Concentrations and Isotopes in Corals and Water near Bermuda, 1780–2000. *Earth Planet. Sci. Lett.* **2009**, *283* (1–4), 93–100.
- (12) Boyle, E. A.; Lee, J.-M.; Echegoyen, Y.; Noble, A.; Moos, S.; Carrasco, G.; Zhao, N.; Kayser, R.; Zhang, J.; Gamo, T.; et al. Anthropogenic Lead Emissions in the Ocean: The Evolving Global Experiment. *Oceanography* **2014**, *27* (1), 69–75.
- (13) Schaule, B. K.; Patterson, C. C. Perturbations of the Natural Lead Depth Profile in the Sargasso Sea by Industrial Lead. In *Trace Metals in Sea Water*; Wong, C. S., Boyle, E., Bruland, K. W., Burton, J. D., Goldberg, E. D., Eds.; 2013; pp 487–503, [DOI: 10.1007/978-1-4757-6864-0\\_29](https://doi.org/10.1007/978-1-4757-6864-0_29).
- (14) Boyle, E. A.; Chapnick, S. D.; Shen, G. T.; Bacon, M. P. Temporal Variability of Lead in the Western North Atlantic. *J. Geophys. Res.* **1986**, *91* (C7), 8573–8593.
- (15) Shen, G. T.; Boyle, E. A. Thermocline Ventilation of Anthropogenic Lead in the Western North Atlantic. *J. Geophys. Res.* **1988**, *93* (C12), 15715–15732.
- (16) Véron, A. J.; Church, T. M.; Patterson, C. C.; Flegal, A. R. Use of Stable Lead Isotopes to Characterize the Sources of Anthropogenic Lead in North Atlantic Surface Waters. *Geochim. Cosmochim. Acta* **1994**, *58* (15), 3199–3206.

- (17) Véron, A. J.; Church, T. M.; Flegal, A. R. Lead Isotopes in the Western North Atlantic: Transient Tracers of Pollutant Lead Inputs. *Environ. Res.* **1998**, *78* (2), 104–111.
- (18) Véron, A. J.; Church, T. M.; Rivera-Duarte, I.; Flegal, A. R. Stable Lead Isotopic Ratios Trace Thermohaline Circulations in the Subarctic North Atlantic. *Deep Sea Res., Part II* **1999**, *46* (5), 919–935.
- (19) Noble, A. E.; Echegoyen-Sanz, Y.; Boyle, E. A.; Ohnemus, D. C.; Lam, P. J.; Kayser, R.; Reuer, M.; Wu, J.; Smethie, W. Dynamic Variability of Dissolved Pb and Pb Isotope Composition from the U.S. North Atlantic GEOTRACES Transect. *Deep Sea Res., Part II* **2015**, *116*, 208–225.
- (20) Wu, J.; Boyle, E. A. Lead in the Western North Atlantic Ocean: Completed Response to Leaded Gasoline Phaseout. *Geochim. Cosmochim. Acta* **1997**, *61* (15), 3279–3283.
- (21) Pinedo-González, P.; West, A. J.; Tovar-Sánchez, A.; Duarte, C. M.; Sañudo-Wilhelmy, S. A. Concentration and Isotopic Composition of Dissolved Pb in Surface Waters of the Modern Global Ocean. *Geochim. Cosmochim. Acta* **2018**, *235*, 41–54.
- (22) Schlitzer, R.; Anderson, R. F.; Dodas, E. M.; Lohan, M.; Geibert, W.; Tagliabue, A.; Bowie, A.; Jeandel, C.; Maldonado, M. T.; Landing, W. M.; et al. The GEOTRACES Intermediate Data Product 2017. *Chem. Geol.* **2018**, *493* (June), 210–223.
- (23) Zurbrick, C. M.; Boyle, E. A.; Kayser, R. J. R.; Reuer, M. K.; Wu, J.; Planquette, H.; Shelley, R.; Boutorh, J.; Cheize, M.; Contreira, L.; et al. Dissolved Pb and Pb Isotopes in the North Atlantic from the GEOVIDE Transect (GEOTRACES GA-01) and Their Decadal Evolution. *Biogeosciences* **2018**, *15* (16), 4995–5014.
- (24) Bridgestock, L.; Rehkämper, M.; van de Flierdt, T.; Paul, M.; Milne, A.; Lohan, M. C.; Achterberg, E. P. The Distribution of Lead Concentrations and Isotope Compositions in the Eastern Tropical Atlantic Ocean. *Geochim. Cosmochim. Acta* **2018**, *225*, 36–51.
- (25) Chen, M.; Boyle, E. A.; Lee, J. M.; Nurhati, I.; Zurbrick, C.; Switzer, A. D.; Carrasco, G. Lead Isotope Exchange between Dissolved and Fluvial Particulate Matter: A Laboratory Study from the Johor River Estuary. *Philos. Trans. R. Soc., A* **2016**, *374* (2081), 20160054.
- (26) Rusiecka, D.; Gledhill, M.; Milne, A.; Achterberg, E. P.; Annett, A. L.; Atkinson, S.; Birchill, A.; Karstensen, J.; Lohan, M.; Mariez, C.; et al. Anthropogenic Signatures of Lead in the Northeast Atlantic. *Geophys. Res. Lett.* **2018**, *45* (6), 2734–2743.
- (27) Zurbrick, C. M.; Gallon, C. C. C.; Flegal, A. R. Historic and Industrial Lead within the Northwest Pacific Ocean Evidenced by Lead Isotopes in Seawater. *Environ. Sci. Technol.* **2017**, *51* (3), 1203–1212.
- (28) Timmermans, M. L.; Garrett, C.; Carmack, E. The Thermohaline Structure and Evolution of the Deep Waters in the Canada Basin, Arctic Ocean. *Deep Sea Res., Part I* **2003**, *50* (10–11), 1305–1321.
- (29) Steele, M.; Morison, J.; Ermold, W.; Rigor, I.; Ortmeyer, M.; Shimada, K. Circulation of Summer Pacific Halocline Water in the Arctic Ocean. *J. Geophys. Res.* **2004**, *109* (C2), C02027.
- (30) McLaughlin, F.; Shimada, K.; Carmack, E.; Itoh, M.; Nishino, S. The Hydrography of the Southern Canada Basin, 2002. *Polar Biol.* **2005**, *28* (3), 182–189.
- (31) Timmermans, M. L.; Proshutinsky, A.; Golubeva, E.; Jackson, J. M.; Krishfield, R.; McCall, M.; Platov, G.; Toole, J.; Williams, W.; Kikuchi, T.; et al. Mechanisms of Pacific Summer Water Variability in the Arctic's Central Canada Basin. *J. Geophys. Res. Ocean.* **2014**, *119* (11), 7523–7548.
- (32) McLaughlin, F. A.; Carmack, E. C.; Macdonald, R. W.; Melling, H.; Swift, J. H.; Wheeler, P. A.; Sherr, B. F.; Sherr, E. B. The Joint Roles of Pacific and Atlantic-Origin Waters in the Canada Basin, 1997–1998. *Deep Sea Res., Part I* **2004**, *51* (1), 107–128.
- (33) Shimada, K.; Itoh, M.; Nishino, S.; McLaughlin, F.; Carmack, E.; Proshutinsky, A. Halocline Structure in the Canada Basin of the Arctic Ocean. *Geophys. Res. Lett.* **2005**, *32* (3), L03605.
- (34) Michel, C.; Ingram, R. G.; Harris, L. R. Variability in Oceanographic and Ecological Processes in the Canadian Arctic Archipelago. *Prog. Oceanogr.* **2006**, *71* (2–4), 379–401.
- (35) Beszczynska-Möller, A.; Woodgate, R.; Lee, C.; Melling, H.; Karcher, M. A Synthesis of Exchanges Through the Main Oceanic Gateways to the Arctic Ocean. *Oceanography* **2011**, *24* (3), 82–99.
- (36) Wang, Q.; Myers, P. G.; Hu, X.; Bush, A. B. G. Flow Constraints on Pathways through the Canadian Arctic Archipelago. *Atmos.-Ocean* **2012**, *50* (s), 373–385.
- (37) Hill, V. J.; Matrai, P. A.; Olson, E.; Suttles, S.; Steele, M.; Codispoti, L. A.; Zimmerman, R. C. Synthesis of Integrated Primary Production in the Arctic Ocean: II. In Situ and Remotely Sensed Estimates. *Prog. Oceanogr.* **2013**, *110*, 107–125.
- (38) Proshutinsky, A.; Bourke, R. H.; McLaughlin, F. A. The Role of the Beaufort Gyre in Arctic Climate Variability: Seasonal to Decadal Climate Scales. *Geophys. Res. Lett.* **2002**, *29* (23), 15-1–15-4.
- (39) Rudels, B. The Outflow of Polar Water through the Arctic Archipelago and the Oceanographic Conditions in Baffin Bay. *Polar Res.* **1986**, *4* (2), 161–180.
- (40) Tang, C. C. L.; Ross, C. K.; Yao, T.; Petrie, B.; DeTracey, B. M.; Dunlap, E. The Circulation, Water Masses and Sea-Ice of Baffin Bay. *Prog. Oceanogr.* **2004**, *63* (4), 183–228.
- (41) Yashayaev, I.; Loder, J. W. Recurrent Replenishment of Labrador Sea Water and Associated Decadal-Scale Variability. *J. Geophys. Res. Ocean.* **2016**, *121* (11), 8095–8114.
- (42) Lozier, M. S.; Bacon, S.; Bower, A. S.; Cunningham, S. A.; Femke de Jong, M. F.; de Steur, L.; deYoung, B.; Fischer, J.; Gary, S. F.; Greenan, B. J. W.; et al. Overturning in the Subpolar North Atlantic Program: A New International Ocean Observing System. *Bull. Am. Meteorol. Soc.* **2017**, *98* (4), 737–752.
- (43) Yashayaev, I.; van Aken, H. M.; Holliday, N. P.; Bersch, M. Transformation of the Labrador Sea Water in the Subpolar North Atlantic. *Geophys. Res. Lett.* **2007**, *34* (22), L22605.
- (44) Kondo, Y.; Obata, H.; Hioki, N.; Ooki, A.; Nishino, S.; Kikuchi, T.; Kuma, K. Transport of Trace Metals (Mn, Fe, Ni, Zn and Cd) in the Western Arctic Ocean (Chukchi Sea and Canada Basin) in Late Summer 2012. *Deep Sea Res., Part I* **2016**, *116*, 236–252.
- (45) Yashayaev, I.; Clarke, A. Evolution of North Atlantic Water Masses Inferred from Labrador Sea Salinity Series. *Oceanography* **2008**, *21* (1), 30–45.
- (46) Curry, B.; Lee, C. M.; Petrie, B. Volume, Freshwater, and Heat Fluxes through Davis Strait, 2004–05\*. *J. Phys. Oceanogr.* **2011**, *41* (3), 429–436.
- (47) Giesbrecht, T.; Sim, N.; Orians, K. J.; Cullen, J. T. The Distribution of Dissolved and Total Dissolvable Aluminum in the Beaufort Sea and Canada Basin Region of the Arctic Ocean. *J. Geophys. Res. Ocean* **2013**, *118* (12), 6824–6837.
- (48) Cutter, G. R.; Andersson, P.; Codispoti, L.; Croot, P.; Francois, R.; Lohan, M. C.; Obata, H.; van der Looff, M. R. *Sampling and Sample-Handling Protocols for GEOTRACES Cruises*, Version 1.0; 2010 Geotraces Standards and Intercalibration Committee, 2010.
- (49) Wu, J.; Boyle, E. A. Low Blank Preconcentration Technique for the Determination of Lead, Copper, and Cadmium in Small-Volume Seawater Samples by Isotope Dilution ICPMS. *Anal. Chem.* **1997**, *69* (13), 2464–2470.
- (50) McAlister, J. A.; Orians, K. J. Dissolved Gallium in the Beaufort Sea of the Western Arctic Ocean: A GEOTRACES Cruise in the International Polar Year. *Mar. Chem.* **2015**, *177* (2015), 101–109.
- (51) Blanke, B.; Arhan, M.; Madec, G.; Roche, S. Warm Water Paths in the Equatorial Atlantic as Diagnosed with a General Circulation Model. *J. Phys. Oceanogr.* **1999**, *29* (11), 2753–2768.
- (52) Hu, X.; Sun, J.; Chan, T. O.; Myers, P. G. Thermodynamic and Dynamic Ice Thickness Contributions in the Canadian Arctic Archipelago in NEMO-LIM2 Numerical Simulations. *Cryosphere* **2018**, *12* (4), 1233–1247.
- (53) Madec, G.; NEMO Team *NEMO Ocean Engine*, Note du Pôle de Modélisation; l'Institut Pierre-Simon Laplace, 2008; Vol. 27, pp 1288–1679.
- (54) Smith, G. C.; Roy, F.; Mann, P.; Dupont, F.; Brasnett, B.; Lemieux, J.-F.; Laroche, S.; Belair, S. A New Atmospheric Dataset for Forcing Ice-Ocean Models: Evaluation of Reforecasts Using the

- Canadian Global Deterministic Prediction System. *Q. J. R. Meteorol. Soc.* **2014**, *140* (680), 881–894.
- (55) Ferry, N.; Parent, L.; Garric, G.; Bricaud, C.; Testut, C.-E.; Galloudec, O. L.; Lellouche, J.-M.; Drevillon, M.; Greiner, E.; Barnier, B.; et al. *GLORYS2V1 Global Ocean Reanalysis of the Altimetric Era (1993–2009) at Meso Scale*; Copernicus Marine Environment Monitoring Service (CMEMS), 2012.
- (56) Dai, A.; Qian, T.; Trenberth, K. E.; Milliman, J. D. Changes in Continental Freshwater Discharge from 1948 to 2004. *J. Clim.* **2009**, *22* (10), 2773–2792.
- (57) Marsay, C. M.; Kadko, D.; Landing, W. M.; Morton, P. L.; Summers, B. A.; Buck, C. S. Concentrations, Provenance and Flux of Aerosol Trace Elements during US GEOTRACES Western Arctic Cruise GN01. *Chem. Geol.* **2018**, *502* (May), 1–14.
- (58) Boyle, E.; Lee, J.-M.; Echegoyen, Y.; Noble, A.; Moos, S.; Carrasco, G.; Zhao, N.; Kayser, R.; Zhang, J.; Gamo, T.; et al. Anthropogenic Lead Emissions in the Ocean: The Evolving Global Experiment. *Oceanography* **2014**, *27* (1), 69–75.
- (59) Proshutinsky, A.; Krishfield, R.; Timmermans, M.-L.; Toole, J.; Carmack, E.; McLaughlin, F.; Williams, W. J.; Zimmermann, S.; Itoh, M.; Shimada, K. Beaufort Gyre Freshwater Reservoir: State and Variability from Observations. *J. Geophys. Res.* **2009**, *114*, C00A10.
- (60) Jackson, J. M.; Carmack, E. C.; McLaughlin, F. A.; Allen, S. E.; Ingram, R. G. Identification, Characterization, and Change of the near-Surface Temperature Maximum in the Canada Basin, 1993–2008. *J. Geophys. Res.* **2010**, *115* (5), C05021.
- (61) Guay, C. K. H.; McLaughlin, F. a.; Yamamoto-Kawai, M. Differentiating Fluvial Components of Upper Canada Basin Waters on the Basis of Measurements of Dissolved Barium Combined with Other Physical and Chemical Tracers. *J. Geophys. Res.* **2009**, *114* (C1), C00A09.
- (62) Lansard, B.; Mucci, A.; Miller, L. A.; MacDonald, R. W.; Gratton, Y. Seasonal Variability of Water Mass Distribution in the Southeastern Beaufort Sea Determined by Total Alkalinity and  $\Delta^{18}\text{O}$ . *J. Geophys. Res. Ocean* **2012**, *117* (C3), C03003.
- (63) Colombo, M.; Brown, K. A.; De Vera, J.; Bergquist, B. A.; Orians, K. J. Trace Metal Geochemistry of Remote Rivers in the Canadian Arctic Archipelago. Accepted for publication, *Chem. Geol.*, May 2019.
- (64) Dai, M. H.; Martin, J. M. First Data on Trace Metal Level and Behaviour in Two Major Arctic River-Estuine Systems (Ob and Yenisey) and in the Adjacent Kara Sea, Russia. *Earth Planet. Sci. Lett.* **1995**, *131* (3–4), 127–141.
- (65) Tanguy, V.; Waeles, M.; Gigault, J.; Cabon, J.-Y.; Quentel, F.; Riso, R. D. The Removal of Colloidal Lead during Estuarine Mixing: Seasonal Variations and Importance of Iron Oxides and Humic Substances. *Mar. Freshwater Res.* **2011**, *62* (4), 329–341.
- (66) Bruland, K. W.; Middag, R.; Lohan, M. C. Controls of Trace Metals in Seawater. *Treatise on Geochemistry*, 2nd ed.; Elsevier, 2013; Vol. 8, pp 19–51, DOI: [10.1016/B978-0-08-095975-7.00602-1](https://doi.org/10.1016/B978-0-08-095975-7.00602-1).
- (67) Yamamoto-Kawai, M.; McLaughlin, F. A.; Carmack, E. C.; Nishino, S.; Shimada, K.; Kurita, N. Surface Freshening of the Canada Basin, 2003–2007: River Runoff versus Sea Ice Meltwater. *J. Geophys. Res.* **2009**, *114* (4), C00A05.
- (68) Measures, C. I. The Role of Entrained Sediments in Sea Ice in the Distribution of Aluminium and Iron in the Surface Waters of the Arctic Ocean. *Mar. Chem.* **1999**, *68* (1–2), 59–70.
- (69) Klunder, M. B.; Bauch, D.; Laan, P.; De Baar, H. J. W.; Van Heuven, S.; Ober, S. Dissolved Iron in the Arctic Shelf Seas and Surface Waters of the Central Arctic Ocean: Impact of Arctic River Water and Ice-Melt. *J. Geophys. Res. Ocean* **2012**, *117* (C1), C01027.
- (70) Marsay, C. M.; Aguilar-Islas, A.; Fitzsimmons, J. N.; Hatta, M.; Jensen, L. T.; John, S. G.; Kadko, D.; Landing, W. M.; Lanning, N. T.; Morton, P. L.; et al. Dissolved and Particulate Trace Elements in Late Summer Arctic Melt Ponds. *Mar. Chem.* **2018**, *204* (June), 70–85.
- (71) Gruber, N.; Sarmiento, J. L. Global Patterns of Marine Nitrogen Fixation and Denitrification. *Global Biogeochem. Cycles* **1997**, *11* (2), 235–266.
- (72) Ardyna, M.; Babin, M.; Gosselin, M.; Devred, E.; Bélanger, S.; Matsuoka, A.; Tremblay, J. E. Parameterization of Vertical Chlorophyll a in the Arctic Ocean: Impact of the Subsurface Chlorophyll Maximum on Regional, Seasonal, and Annual Primary Production Estimates. *Biogeosciences* **2013**, *10* (6), 4383–4404.
- (73) Brown, Z. W.; Van Dijken, G. L.; Arrigo, K. R. A Reassessment of Primary Production and Environmental Change in the Bering Sea. *J. Geophys. Res.* **2011**, *116* (C8), C08014.
- (74) Lopore, K.; Moran, S. B.; Smith, J. N.  $^{210}\text{Pb}$  as a Tracer of Shelf-Basin Transport and Sediment Focusing in the Chukchi Sea. *Deep Sea Res., Part II* **2009**, *56* (17), 1305–1315.
- (75) Chen, M.; Ma, Q.; Guo, L.; Qiu, Y.; Li, Y.; Yang, W. Importance of Lateral Transport Processes to  $^{210}\text{Pb}$  Budget in the Eastern Chukchi Sea during Summer 2003. *Deep Sea Res., Part II* **2012**, *81*–84, 53–62.
- (76) Hioki, N.; Kuma, K.; Morita, Y.; Sasayama, R.; Ooki, A.; Kondo, Y.; Obata, H.; Nishioka, J.; Yamashita, Y.; Nishino, S.; Kikuchi, T.; Aoyama, M. Laterally Spreading Iron, Humic-like Dissolved Organic Matter and Nutrients in Cold, Dense Subsurface Water of the Arctic Ocean. *Sci. Rep.* **2015**, *4*, 6775.
- (77) Granger, J.; Sigman, D. M.; Gagnon, J.; Tremblay, J.-E.; Mucci, A. On the Properties of the Arctic Halocline and Deep Water Masses of the Canada Basin from Nitrate Isotope Ratios. *J. Geophys. Res.: Oceans* **2018**, *123*, 5443–5458.
- (78) Kuzyk, Z. Z. A.; Gobeil, C.; Macdonald, R. W.  $^{210}\text{Pb}$  and  $^{137}\text{Cs}$  in Margin Sediments of the Arctic Ocean: Controls on Boundary Scavenging. *Global Biogeochem. Cycles* **2013**, *27* (2), 422–439.
- (79) Vieira, L. H.; Achterberg, E. P.; Scholten, J.; Beck, A. J.; Liebetrau, V.; Mills, M. M.; Arrigo, K. R. Benthic Fluxes of Trace Metals in the Chukchi Sea and Their Transport into the Arctic Ocean. *Mar. Chem.* **2019**, *208*, 43–55.
- (80) Nozaki, Y.; Zhang, J.; Takeda, A.  $^{210}\text{Pb}$  and  $^{210}\text{Po}$  in the Equatorial Pacific and the Bering Sea: The Effects of Biological Productivity and Boundary Scavenging. *Deep Sea Res., Part II* **1997**, *44* (9), 2203–2220.
- (81) Tanhua, T.; Jones, E. P.; Jeansson, E.; Jutterström, S.; Smethie, W. M.; Wallace, D. W. R.; Anderson, L. G. Ventilation of the Arctic Ocean: Mean Ages and Inventories of Anthropogenic CO<sub>2</sub> and CFC-11. *J. Geophys. Res.* **2009**, *114* (1), C01002.
- (82) Macdonald, R. W.; Carmack, E. C.; Wallace, D. W. R. Tritium and Radiocarbon Dating of Canada Basin Deep Waters. *Science (Washington, DC, U. S.)* **1993**, *259* (5091), 103–104.
- (83) Cuny, J.; Rhines, P. B.; Kwok, R. Davis Strait Volume, Freshwater and Heat Fluxes. *Deep Sea Res., Part I* **2005**, *52* (3), 519–542.
- (84) Yashayaev, I.; Loder, J. W. Enhanced Production of Labrador Sea Water in 2008. *Geophys. Res. Lett.* **2009**, *36* (1), L01606.
- (85) Yashayaev, I.; Bersch, M.; van Aken, H. M. Spreading of the Labrador Sea Water to the Irminger and Iceland Basins. *Geophys. Res. Lett.* **2007**, *34* (10), L10602.
- (86) Cuny, J.; Rhines, P. B.; Niiler, P. P.; Bacon, S. Labrador Sea Boundary Currents and the Fate of the Irminger Sea Water. *J. Phys. Oceanogr.* **2002**, *32* (2), 627–647.
- (87) Azetsu-Scott, K.; Jones, E. P.; Gershey, R. M. Distribution and Ventilation of Water Masses in the Labrador Sea Inferred from CFCs and Carbon Tetrachloride. *Mar. Chem.* **2005**, *94* (1–4), 55–66.
- (88) Grenier, M.; Francois, R.; Soon, M.; Baconnais, I.; Pham, V.; Jeandel, C. Ocean Circulation and Land-Ocean Exchanges off the North Eastern Canadian Coasts as Told by Dissolved Geochemical Tracers. *Goldschmidt Abstr.* **2018**, 880.
- (89) Hayes, C. T.; Anderson, R. F.; Fleisher, M. Q.; Huang, K. F.; Robinson, L. F.; Lu, Y.; Cheng, H.; Edwards, R. L.; Moran, S. B.  $^{230}\text{Th}$  and  $^{231}\text{Pa}$  on GEOTRACES GA03, the U.S. GEOTRACES North Atlantic Transect, and Implications for Modern and Paleoceango-graphic Chemical Fluxes. *Deep Sea Res., Part II* **2015**, *116*, 29–41.
- (90) Hannah, C. G.; Dupont, F.; Dunphy, M. Polynyas and Tidal Currents in the Canadian Arctic Archipelago. *Arctic* **2009**, *62* (1), 83–95.

- (91) Hughes, K. G.; Klymak, J. M.; Williams, W. J.; Melling, H. Tidally Modulated Internal Hydraulic Flow and Energetics in the Central Canadian Arctic Archipelago. *J. Geophys. Res.: Oceans* **2018**, *123* (8), 5210–5229.
- (92) Lenaerts, J. T. M.; Van Angelen, J. H.; Van Den Broeke, M. R.; Gardner, A. S.; Wouters, B.; Van Meijgaard, E. Irreversible Mass Loss of Canadian Arctic Archipelago Glaciers. *Geophys. Res. Lett.* **2013**, *40* (5), 870–874.
- (93) Kanna, N.; Sugiyama, S.; Ohashi, Y.; Sakakibara, D.; Fukamachi, Y.; Nomura, D. Upwelling of Macronutrients and Dissolved Inorganic Carbon by a Subglacial Freshwater Driven Plume in Bowdoin Fjord, Northwestern Greenland. *J. Geophys. Res.: Biogeosci.* **2018**, *123*, 1666–1682.